Design of Origami-Based Mechanisms in Monolithic Thick-Sheet Materials using an Optimization Approach

Nathan Pehrson
Compliant Mechanisms Research
Department of Mechanical Engineering
Brigham Young University
Provo, Utah 84606
Email: napehrson@byu.edu

Joseph Stack
Department of Mechanical Engineering
Brigham Young University
Provo, Utah 84606
Email: jstack14@byu.net

April 19, 2017

Abstract

Design of origami-based mechanisms in monolithic thick-sheet materials using compliant mechanisms as joints is a recent approach in folding materials. Single-fold fold patterns can be designed using existing design techniques. However, multi-fold fold patterns may increase the complexity of the design process of such mechanisms causing the process to become impractical and cumbersome. Proposed here is an optimization approach which can automate the design of complex fold patterns.

1 Introduction

Recent interest in origami-based engineering design has illuminated opportunities for new developments and has also introduced many challenges. One such challenge is the inability to fold engineering materials which tend to be thick compared to the fold patterns which assume zero thickness. Several approaches have been developed to accommodate the thickness of materials [1, 2, 3]. A unique method to accommodate the thickness of materials in origami engineering has been proposed [4] and is called the strained joint method. This allows for folding of the material without assembly of its panels and joints (see Figure 1).

Figure 1: An example of folding a monolithic thick-sheet material using the strained joint method.

This fabrication out of monolithic thick-sheet materials is viable due to the incorporation of compliant mechanisms formed, termed surrogate folds. To obtain large angular deflections required for many origami folds, certain surrogate folds are particularly beneficial, especially when area is to be conserved. These particular surrogate folds are named Lamina Emergent Torsion (LET) joints, one of which is shown in Figure 2. This figure shows a LET joint and a cut away cross section, indicating a bar in torsion as the shaded area. To accommodate large deflections [5], surrogate folds can be formed in series and in parallel. Greater amounts of deflection can be achieved when surrogate folds are placed in series, and greater amounts of stiffness results when placed in parallel.

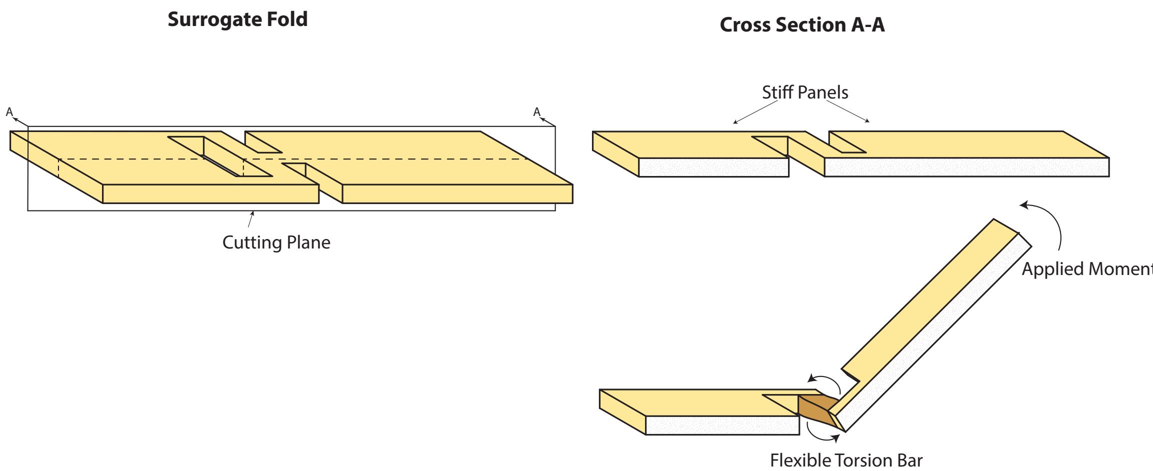

Figure 2: An example of a surrogate fold that uses torsion of members that lie on the axis of rotation of the joint.

A unique collection of folds and panels which result in an origami model is its fold pattern. To describe the geometry and kinematics of fold patterns, a zero-thickness assumption is often used to simplify models, allowing origami artists and designers to represent finite materials (such as paper) as infinitesimally thin planes and lines.

For monolithic thick-sheet materials the strained joint method relies upon flexible regions (not lines) of material to gain its motion between panels. Accordingly, in place of folds and fold patterns there are joint areas and joint patterns, where a joint area represents the 2D area containing the joint, with the assumption that the third dimension (material thickness) remains constant (Figure 3).

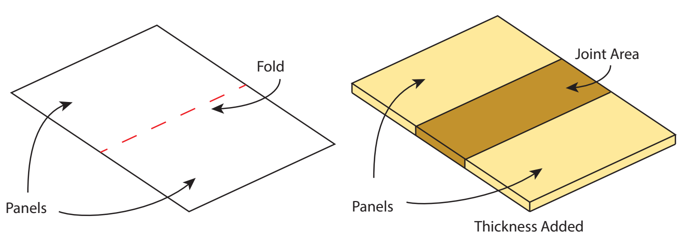

Figure 3: A fold indicated by a dotted line (left), and joint area indicated by darkly shaded region (right), both enabling rotation of the panels on either side.

Exterior vertices (like that of folding a piece of paper in half) are the simplest of origami fold patterns and the use of compliant mechanisms as surrogate folds for these patterns have been discussed in detail by Delimont et al. [6]. However, the discussion has been limited to exterior vertices. Here, the discussion is broadened to include more complex patterns of exterior *and* interior vertices (where multiple fold lines meet at a point). However, due to interference of joints at one or more vertices for complex patterns, an optimization of joints throughout a monolithic thick-sheet material is explored.

1.1 Application

High stowed volume efficiencies for deployable solar array structures is a NASA space mission enabling technology [7]. Generally, for a constant photovoltaic (PV) cell efficiency and solar irradiation, the amount of power possible in solar cell power generation is a function of the surface area of the PV cells of an array; an increase in power generation requires an increase in area. In spaceflight, the stowed volume and spacecraft mass must remain low to feasibly launch these systems from earth into space. Maneuverability of spacecraft once in space is improved with low mass. Furthermore, deployable structures, such as solar arrays, must have adequate strength and stiffness to undergo spacecraft maneuvers and pointing to face towards the sun. They must be reliable in their deployment and, if applicable, retraction.

So, from a system-architecture view, the target of attaining higher solar power generation can be stated as this: a greater amount of PV cell area using a deployable strong and stiff structure with low mass and low stowed volume creates higher solar power generation which enables new space missions. To motivate the design of these folding systems, we will consider the needs of this application as we use optimization as a design tool. These needs include foldability, deployability, maximizing usable area, and maintaining target stiffnesses.

2 Optimization Techniques

2.1 Objective Function

The optimization attempts to minimize the joints areas in a multi-vertex fold pattern. This objective is relevant for applications of origami based designs because joint areas often become unusable for the purposes of the function which the remaining panels perform. Constraints on these folds require that the material does not yield, a target stiffness for each joint is met, that the joints allow for proper layering, and that the optimization results in non-negative real values for the lengths of the torsion bars. The primary input parameter to the optimization is a folding pattern containing one or more vertices with one or more folds at each vertex. Additional inputs include material properties, the thickness of the monolithic sheet, a cut width and a minimum stiffness for each joint. The result of the optimization is useful for determining the total area required for each hinge to ensure all critical constraints are meet. The optimization problem is defined formally as:

$$\begin{aligned} \text{minimize} \quad & A(x) \\ \text{with respect to} \quad & x \\ \text{subject to} \quad & c_{stress}(x) \leq 0 \\ & c_{stiffness}(x) \leq 0 \\ & c_{layering}(x) \leq 0 \\ & c_{length}(x) \leq 0 \end{aligned} \tag{1}$$

Where the objective function $A(x)$ is the sum of areas of each joint.

2.2 Constraints

A common engineering constraint is one against failure of the material. Here we consider the maximum stress experienced in the joints to be the maximum shear stress in the torsion bars and for conservative design, we use the maximum shear stress failure theory, scaled:

$$c_{stress}(x) = \frac{2\tau_{max,i}SF - \sigma_Y}{\sigma_Y} \tag{2}$$

A competing constraint to the stress constraint is the joint stiffness constraint. Here we constrain the stiffness of each joint to be above a minimum, again, scaled. This constraint encourages a global stiffness of the mechanism to be above some threshold for stability.

$$c_{stiffness}(x) = \frac{K_{min,i} - K_i}{K_{min,i}} \tag{3}$$

Another constraint on the problem is a layering constraint. Each joint in the fold pattern has two panels. When the whole pattern is folded, these panels will stack on top of one another. Some panels will span no layers (the panels on a joint are touching each other) while others will span multiple panels. The layering constraint defines how wide the joint needs to be to have enough material to span the required number of panels. Equation 4 defines the constraint in terms of the required width of the joint W_r and the actual width W_a. Equation 5 defines the required width with the layer numbers of each panel on the joint l_n, material thickness t, fold angle γ and a cushion factor of $\alpha_c = 1.1$ to compensate for ease of folding.

$$c_{layering}(x) = \frac{W_{r,i} - W_{a,i}}{W_{r,i}} \tag{4}$$

To accommodate fold angles $0 \leq \gamma \leq 180$ two cases must be considered. When $\gamma < 180$, the fold has a straight portion that spans intermediate layers as shown in the right image of Figure 4. Then the fold wraps around the layered components to the appropriate angle. When $\gamma = 180$ as shown on the left of Figure 4, one less layer is spanned. As a result the function for the required width is piecewise based on the fold angle.

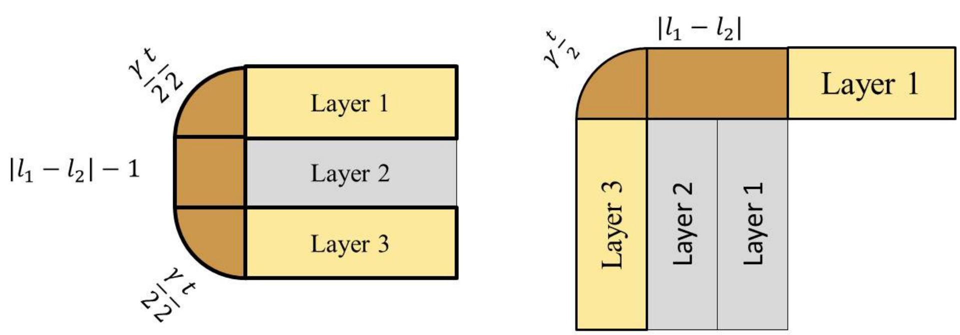

Figure 4: Left: Layering problem for angle equal to 180 deg. Right: Layering problem for angles less than 180 deg.

Equation 5 shows the function for determining the required width of the fold. Equation 6 shows the piecewise function for n based on the fold angle γ.

$$W_{r,i} = \alpha_c t(\frac{\gamma}{2} + n) \tag{5}$$

$$n(\gamma) = \begin{cases} |l_{n_1} - l_{n_2}| - 1 & \text{for} \quad \gamma = 180 \ \& \ |l_{n_1} - l_{n_2}| > 0 \\ |l_{n_1} - l_{n_2}| & \text{for} \quad \gamma < 180 \\ \textit{unsupported} & \text{for} \quad \textit{otherwise} \end{cases} \tag{6}$$

Figure 5 shows the new cases of folded panels (oblique fold angles with nested panels). This figure also shows a combination of fold angles; Figure 5(b) shows a 180 degree fold with no nested panels, and Figures 5(a) and 5(c) show fold angles of 72 degrees with varying numbers of panels nested.

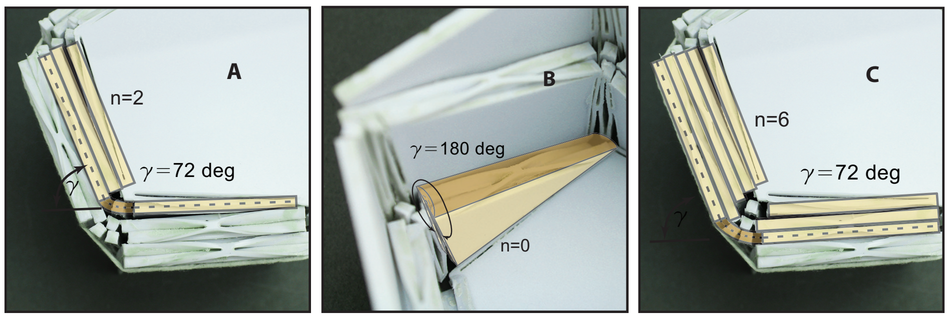

(a) (b) (c)

Figure 5: (a,b,c) Depictions of panels for three joints overlaid on views of the flasher pattern in its stowed state from Figure 8.

One of the difficulties associated with this problem is the high dimensionality. Each joint introduces three design variables and three non-linear and non-continuous constraints. The complexity is due to the discrete nature of the problem coupled with the competing nature of the stress and stiffness constraints. The constraints outlined above result in a feasible region that is very complex and has particular properties that make optimization difficult. Figure 6 shows the feasibility space for one joint of a sample fold pattern. This figure is based on the optimized solution from the Genetic Algorithm for the fold pattern shown and varies the three design variables for joint number 3. The contained volume illustrates the volume that violates no constraints. One of the challenges with this feasibility space is that mutations and reproductions in the genetic algorithm on the series and parallel constraints can cause drastic affects on the feasibility due to the sensitivity of the number of series and parallel members for a given joint. When this is applied on a problem of high dimensionality (many joints) a large population and large number of iterations is required for convergence.

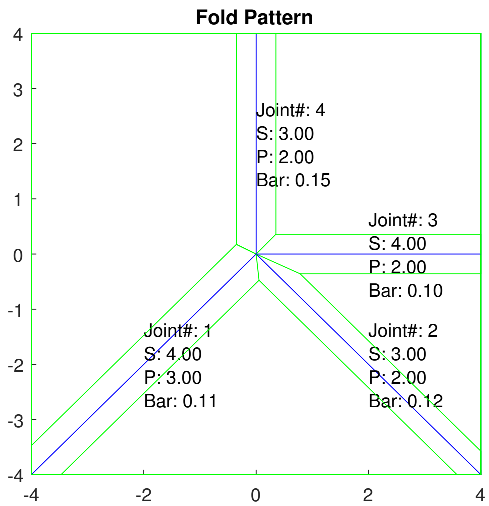

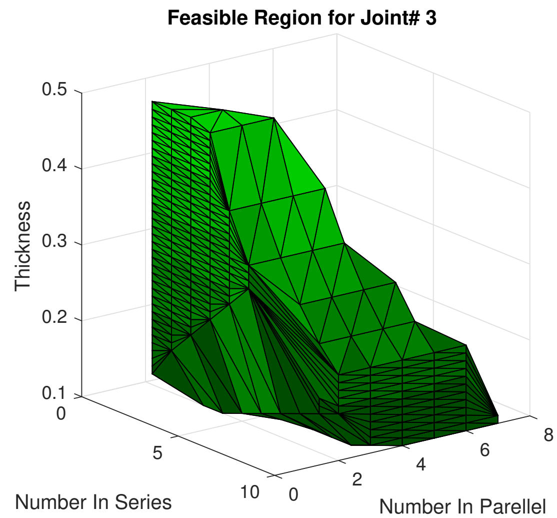

Figure 6: Left: Fold pattern constraint feasibility space is based on. Right: The 3-D feasibility space for number of series, number of parallel, and torsion bar width for joint 3. All other joints are held constant. The feasibility space is the space where no constraints are violated.

2.3 Genetic Algorithm with Mixed Integers

The optimization technique best suited for this application is a genetic algorithm that accommodates mixed integers. This technique is ideal because of the inherently discrete nature of the problem. For each joint in a given fold pattern there are three design variables: the number of segments in series, the number of segments in parallel, and the thickness of the torsion bar. The first two are positive integers and the third value is a positive real number. MATLAB's genetic algorithm method in the Global Optimization Toolbox is used in this report because of it's support for mixed integers optimization with upper and lower bounds.

3 Results

3.1 Square Twist

The square twist fold pattern was used to test this approach. The final fold pattern is shown in Figure 7 and the design variables for this solution are found in Table 1. The total constraint values are summarized in Table 2. The objective function value (the joint area) was 1.6193 (in^2), and the optimization converged on this solution in 6900 function calls. These results were achieved with integer bounds of [1,10] for series and parallel and continuous bounds of [.1,.5] for torsion bar width at each joint. The genetic algorithm had a function tolerance of 1e-5, a constrain tolerance of 1e-5, and a population size of 360.

Table 1: Design variables for an optimized solution to the square twist problem.

Joint	1	2	3	4	5	6	7	8	9	10	11	12
Number in Series	3	3	3	2	3	3	3	3	3	2	3	3
Number in Parallel	1	1	1	2	1	1	2	1	1	1	1	3
Torsion Bar Width	.16	.28	.21	.10	.18	.16	.11	.18	.28	.18	.18	.10

Table 2: Constraint values for an optimized solution to the square twist problem.

Joint	1	2	3	4	5	6	7	8	9	10	11	12
Stress	-0.2	-0.2	-0.3	0.0	-0.3	-0.2	-0.1	-0.3	-0.2	-0.2	-0.3	-0.1
Stiffness	-2.5	-7.8	-3.4	-5.7	-2.4	-3.1	-4.7	-2.5	-7.4	-3.1	-2.4	-7.2
Layer	-0.5	-0.0	-0.7	-0.2	-0.1	-0.5	-0.4	-0.6	-0.0	-0.3	-0.1	-0.3
Minimum Length	-2.6	-2.5	-3.4	-1.5	-3.0	-2.3	-1.5	-3.1	-2.7	-4.3	-3.1	-1.3

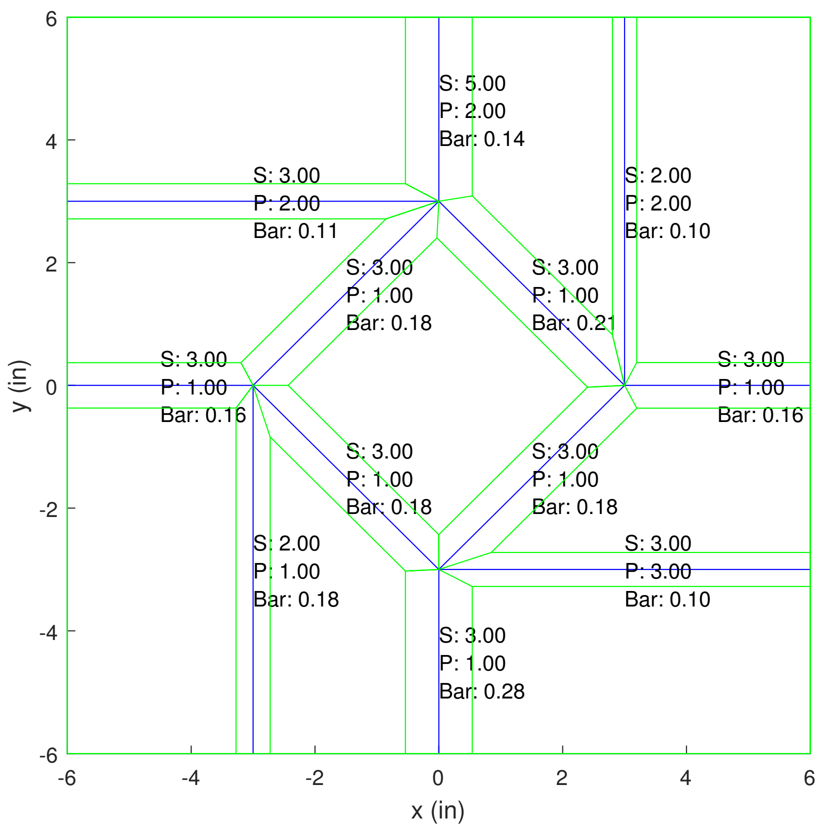

Figure 7: The optimized fold pattern for the square twist problem.

3.2 Flasher

The flasher pattern is as scalable pattern of multiple "rings" that span around an inner shape. In this case, we have one ring that wraps around an inner pentagon. An example of this with 2 rings around a pentagon is shown in Figure 8. This pattern has fold angles of 180, 90 and 72. This allows us to test our layering constraint formulation for varying angles as well as as fold angles that span multiple layers.

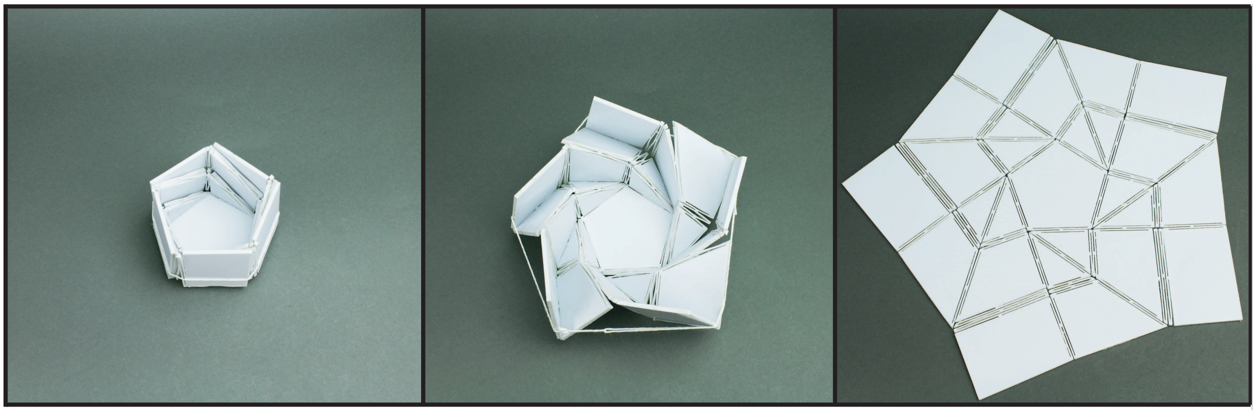

Figure 8: An example of a flasher origami pattern cut from $\frac{1}{8}$ in. thick polypropylene unfolding from its (left to right) stowed, intermediate, and deployed configurations.

The results of the optimization are shown below. The final fold patterns is shown in Figure 9 and the design variables for this solution are found in Table 3. The total constraint violations are summarized in Table 4. The objective function value (the joint area) was .9873 (in^2), and the optimization converged on this solution in 22 generations and 16561 function calls. These results were achieved with integer bounds of [1,6] for series and parallel and continuous bounds of [.1,.3] for torsion bar width at each joint. The genetic algorithm had a function tolerance of 1e-6, a constrain tolerance of 1e-5, and a population size of 720.

Table 3: Design variables for an optimized solution to the flasher problem.

Joint	1	2	3	4	5	6	7	8	9	10
Number in Series	3	3	4	4	4	3	4	4	2	5
Number in Parallel	3	3	4	3	4	3	4	3	3	4
Torsion Bar Width	0.15	0.18	0.12	0.15	0.12	0.19	0.25	0.18	0.27	0.12
Joint	11	12	13	14	15	16	17	18	19	20
Number in Series	4	4	3	3	5	4	6	2	4	3
Number in Parallel	4	3	2	3	3	3	4	3	4	3
Torsion Bar Width	0.12	0.14	0.17	0.16	0.22	0.10	0.17	0.16	0.22	0.18

Table 4: Constraint values for an optimized solution to the flasher problem.

Joint	1	2	3	4	5	6	7	8	9	10
Stress Constraint	-0.14	-0.04	-0.12	-0.09	-0.13	-0.03	-0.14	-0.07	-0.06	-0.08
Stiffness Constraint	-1.04	-0.89	-1.29	-0.09	-1.17	-1.04	-3.43	-0.61	-5.48	-0.26
Layer Constraint	-0.53	-0.62	-0.60	-0.72	-0.62	-0.66	-1.11	-0.86	-0.55	-0.81
Minimum Length Constraint	-0.58	-0.58	-0.03	-0.62	-0.21	-0.86	-0.09	-0.29	-0.15	-0.37
Joint	11	12	13	14	15	16	17	18	19	20
Stress Constraint	-0.05	-0.08	-0.12	-0.02	-0.12	-0.16	-0.17	-0.01	-0.14	-0.13
Stiffness Constraint	-0.38	-0.10	0.27	-0.68	-0.40	0.20	-0.71	-2.61	-2.18	-1.16
Layer Constraint	-0.60	-0.71	-0.58	-0.54	-1.31	-0.66	-1.42	-0.45	-1.13	-0.74
Minimum Length Constraint	-0.46	-0.35	-1.31	-0.81	-0.52	-0.48	-0.16	-0.47	-0.18	-0.69

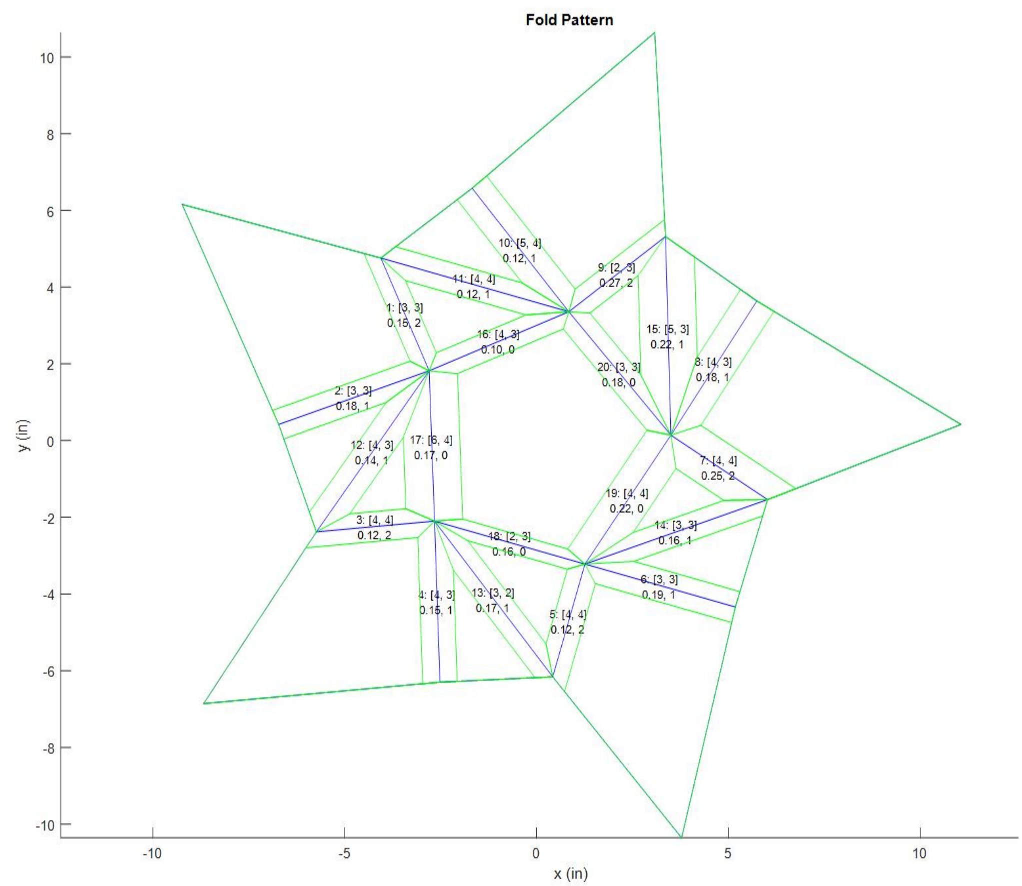

Figure 9: The optimized fold pattern for the flasher problem.

4 Discussion

This optimization-based design approach provides a good solution to the single vertex, square twist, and flasher problems. Constraints have been met allowing for elastic behavior of the folding motion, attainable target required for a good design. As shown in Table 2, the square twist does not violate the stress, stiffness, or layering constraints which shows the design is viable. The same is true for the flasher problem. Despite meeting the constraints and converging to a solution, the design is not perfect. The optimal square twist and flasher design should have symmetry on joints that are similar, however, the solution the optimizer converged on is non-symmetric. Limiting the design variables to only unique joints would prevent this issue, then those variables would be mapped to multiple joints that are symmetric. This approach would ensure a symmetric result and also reduce the number of variables improving the algorithms efficiency.

One limitation with the formulation of the outlined optimization approach is the fixed requirement that each series segment in a joint has the same number of segments in parallel. As the number of series increases, and as a result the tip of each joint grows, the length of the outermost segments shortens. This causes the stress in these members to spike much higher than the more central segments. As a result, the feasible space is drastically changed from what could be feasible if each segment in series could have varying numbers of parallel segments. Unfortunately, this would end up adding an additional parallel constraint for each segment in series on a fold, which would result in dynamically changing the dimensionally of the problem. In context of thick monolithic sheets this issue is especially pronounced. One way for the optimizer to reduce stress is to add increasing number of series joints, however, due to the coupling with parallel constraints this actually can cause an increase in stress. Including this functionality would increase the complexity of the project and reduce the likelihood of convergence in a reasonable time.

5 Conclusions

The results of this project show that the use of a genetic algorithm optimization can aid the design of origami-based mechanisms in monolithic thick-sheet materials. This is especially useful when designing complex fold patterns-patterns with arbitrarily many interior vertices and fold angles, which we have demonstrated.

Current limitations to this work include non-symmetric solutions and the artificial constraint of maintaining the same number of joints in parallel for every row in series. Possible approaches for remedy these limitations have been suggested.

The objective function of our optimization algorithm here was to reduce the joint areas, and thus increase usable panel areas. We showed that we could satisfy the constraints of stress, stiffness, and of layering of panels, indicating that this method can assist in the design of mechanisms for applications such as the space solar array discussed. Automation of these types of mechanisms can speed up design, fabrication, and testing of such mechanisms, pushing the state of the art of folding thick-sheet origami-based monolithic mechanisms forward.

References

[1] T. G. Nelson, R. J. Lang, N. A. Pehrson, S. P. Magleby, and L. L. Howell, "Facilitating deployable mechanisms and structures via developable lamina emergent arrays," *Journal of Mechanisms and Robotics-Transactions of the Asme*, vol. 8, no. 3, 2016.

[2] S. A. Zirbel, R. J. Lang, M. W. Thomson, D. A. Sigel, P. E. Walkemeyer, B. P. Trease, S. P. Magleby, and L. L. Howell, "Accommodating thickness in origami-based deployable arrays," *Journal of Mechanical Design*, vol. 135, no. 11, p. 111005, 2013.

[3] J. S. Ku and E. D. Demaine, "Folding flat crease patterns with thick materials," *Journal of Mechanisms and Robotics*, vol. 8, no. 3, p. 031003, 2016.

[4] N. A. Pehrson, S. P. Magleby, R. J. Lang, and L. L. Howell, "Introduction of monolithic origami with thick-sheet materials," in *International Association for Shell and Spatial Structures*. International Association of Shells and Spatial Structures, September 26-30 2016.

[5] P. N. Russell-Clarke and M. S. Nasher, "Interlocking flexible segments formed from a rigid material," Aug. 22 2013, uS Patent App. 13/768,943. [Online]. Available: https://www.google.com/patents/US20130216740

[6] I. L. Delimont, S. P. Magleby, and L. L. Howell, "A family of dual-segment compliant joints suitable for use as surrogate folds," *Journal of Mechanical Design*, vol. 137, no. 9, 2015.

[7] (2015) Technology area 3: 3.1.3 solar. NASA Technology Roadmaps. [Online]. Available: https://www.nasa.gov/offices/oct/home/roadmaps/index.html